

# Influence of pore size on tensile strength, permeability and porosity of hyaluronan-collagen scaffolds

Amir A. Al-Munajjed · Matthias Hien ·  
Richard Kujat · John P. Gleeson · Joachim Hammer

Received: 6 January 2008 / Accepted: 29 February 2008 / Published online: 18 March 2008  
© Springer Science+Business Media, LLC 2008

**Abstract** Recent investigations have shown the importance of scaffold pore size on the realisation of tissue engineered cartilage which promotes cell adhesion, proliferation and differentiation. The objective of this study was to investigate the influence of pore size on the mechanical properties, the permeability and the porosity of hyaluronan-collagen scaffolds. Hyaluronan-collagen scaffolds with three different mean pore sizes (302.5, 402.5 and 525  $\mu\text{m}$ ) have been produced according to a standardised protocol. The maximum stress at rupture, the Young's Moduli, permeability and porosity of the scaffolds were investigated. The permeability was determined both empirically and mathematically. Increased pore sizes indicated a larger stress at rupture as well as increased Young's Moduli. Porosity and permeability were raised by increasing pore sizes. The mathematically calculated permeability showed the same trend. The results indicate a higher mechanical stability for scaffolds with larger pores. The experimental and mathematical experiments both show increased permeability and fluid mobility for larger pores in scaffolds. Morphological changes resulting from the alteration of pore size led to non-correlation between the calculated and the experimental permeability.

A. A. Al-Munajjed · M. Hien · J. Hammer  
Labor für Werkstofftechnik und Metallographie, University  
of Applied Sciences Regensburg, Regensburg, Germany

*Present Address:*

A. A. Al-Munajjed (✉) · J. P. Gleeson  
Department of Anatomy, Royal College of Surgeons in Ireland,  
123 St. Stephens Green, Dublin 2, Ireland  
e-mail: aalmunajjed@rcsi.ie

R. Kujat  
Department of Surgery, University of Regensburg,  
Regensburg, Germany

## 1 Introduction

The repair of musculoskeletal tissue defects, e.g. cartilage, bone, tendon, muscle, nerve, skin, is still a challenging clinical problem [1]. In particular cartilage does not repair spontaneously due to the absence of blood supply and its dense extracellular matrix with sparsely embedded chondrocytes [2]. In the recent years tissue engineering (TE) has attempted to solve this problem using cell seeded scaffolds, incubated in a bioreactor. Chemical, physical and biological properties are essential for scaffold materials. Scaffolds designed for cell seeding should provide a 3-D and highly porous structure to support cell attachment, proliferation and ECM production [3]. The scaffold material has to be biocompatible and degradable to facilitate cell attachment, proliferation and differentiation due to its surface chemistry [4]. Sufficient mechanical properties are a prerequisite for implantations at load bearing locations [4]. In addition to the mechanical stability, permeability of the scaffold or 3-D construct used for TE application is important as it controls the migration of cells into the scaffolds as well as the diffusion of nutrients and waste in and out of the scaffold [3]. A well-established parameter is the Darcy's constant to describe the permeability of various materials [3, 5]. Permeability ( $k$ , units of  $\text{m}^2$ ) is the fluid conductivity of a porous material and is an important and quantitative parameter describing the scaffold structure independent of sample size and the fluid used and can be expressed mathematically as below [3, 6].

$$k = \frac{Q \cdot l \cdot \mu}{\Delta P \cdot A} \quad (1)$$

The fluid mobility or Darcy's permeability constant ( $K$ , units of  $\text{m}^4/\text{Ns}$ ) is a further important property that defines the fluid flow through porous materials and is calculated by the

volumetric flow rate ( $Q$ ), the length of the specimen ( $l$ ), the sample cross-sectional area, the pressure difference across the scaffold ( $\Delta P$ ) and the viscosity of the fluid ( $\mu$ ) [3]. O'Brien et al. [5, 7] investigated the effect of pore size on permeability in collagen and glycosaminoglycan (CG copolymers) scaffolds produced by freeze drying by measuring and calculating the Darcy's constant [5]. These scaffolds have been developed for skin regeneration with FDA approval and were then adapted for bone TE [5, 7–9]. The investigation showed that the scaffold pores need to be large enough to allow cells to migrate into the structure (about 20  $\mu\text{m}$ ), but small enough (about 120  $\mu\text{m}$ ) to establish a sufficiently high specific surface area [3, 5]. However, there are other parameters like the interconnectivity of the pores that are responsible for mass transport of oxygen and nutrients throughout the scaffold.

Previous investigations for cartilage repair have shown that scaffolds of esterified hyaluronic acid and collagen support the osteochondral differentiation of bone marrow-derived mesenchymal progenitor cells [1, 10, 11]. These novel developed scaffolds were especially designed for TE purposes with a higher collagen concentration (25 mg/ml) for improved mechanical stiffness and cell supportive environment [1]. The matrix stability is achieved by the esterified hyaluronan part, which allows in vivo differentiation of mesenchymal cell progenitor cells [12, 13]. Gelatin was introduced in the matrix as a second part. Gelatin is described in the literature as superior to fibrillar collagen as a substrate for cell attachment, proliferation and differentiation [14, 15]. Therefore, this scaffold uses the advantages of both, collagen and hyaluronan for stability, cell attachment and proliferation [11].

Hyaluronic-collagen scaffolds were investigated concerning chemical, physical and biological properties [1, 11, 16–19]. The target of this investigation is to analyse the influence of pore size (salt grain size 250–354, 354–450 and 450–600  $\mu\text{m}$ ) on (i) the mechanical properties in tension, (ii) the experimental and analytical permeability and (iii) the porosity of the scaffolds.

## 2 Material and methods

### 2.1 Scaffold fabrication

The fabrication of the scaffolds has been previously described [1, 10, 17]. Briefly three different scaffold structures were used in this investigation (Table 1). The

**Table 1** Survey of the used scaffold structure geometries

	Scaffold A ( $\mu\text{m}$ )	Scaffold B ( $\mu\text{m}$ )	Scaffold C ( $\mu\text{m}$ )
Salt crystals	250–355	355–450	450–600
Mean pore size	302.5	402.5	525

basic component of both materials is a spongy matrix consisting of 70% esterified hyaluronan and 30% collagen [10]. The hyaluronan was obtained from a commercially available product (Jaloskin, Fidia Advanced Biopolymers Srl, Italy) which is highly esterified with benzyl alcohol on the free carboxyl groups of glyceronic acid along the polymer. The second compound, type I collagen from gelatin origin was purified by acidic and basic hydrolysis as well as controlled enzymatic treatment with pepsin, according to a standardised industrial protocol [10].

The scaffold components were mixed and air-dried after addition of NaCl crystals with a size of 0.25–0.35, 0.35–0.45 or 0.45–0.60 mm. Before drying, the scaffolds were submerged with Synperonic, a non-ionic tenside, which is also used to control foam manufacturing processes. Finally, the salt was leached out with water, and the composite was dried at room temperature. The size of the salt crystals defines the dimensions of the matrix primary porosity (250–350, 350–450 or 450–600  $\mu\text{m}$ ) as shown in Fig. 1. Due to the drying process, both macro and micro cracking between the primary pores is induced. These cracks are defined as secondary pores within the cell walls of the primary pores. The primary pores provide the location for growth of the embedded cells. The secondary pores generate network along which nutrition flow takes place. Rods of all hyaluronan-collagen matrices were manufactured in dimensions of  $\sim 50$ -mm length and 6-mm diameter. The rods were trimmed into peaces of 5-mm length each.

### 2.2 Tensile tests

Tensile tests were performed on a uniaxial testing system Inspect Desk 50 kN, Hegewald und Peschke<sup>®</sup> Meß- und Prüftechnik GmbH (Nossen, Germany) with a 20 N load cell (accuracy of  $\pm 0.001$  N). All samples were fixed with dental epoxy resin onto two aluminium discs as previously described [1, 19]. The scaffolds were immersed in 0.9% NaCl solution and evacuated for 15 min using a vacuum chamber. Individual geometries of the scaffolds were measured using a microscope (Olympus SZX12 with camera colour view 12) to calculate stress and strain values. The samples were attached under no-strain conditions with the aluminium discs to the machine set-up (Fig. 2). The scaffolds were tested in longitudinal direction. After a preload of 0.1 N, the strain rate was  $0.2 \text{ min}^{-1}$ . Rupture stress and tensile modulus between 0 and 10% were used to describe the mechanical properties of the scaffolds as previously described [1, 19].

## 3 Permeability

### 3.1 Experimental permeability

The permeability of the scaffolds was measured using an experimental device. A schematic view of the device is

**Fig. 1** Scaffolds with pore sizes of 250–355, 355–450 and 450–600 μm

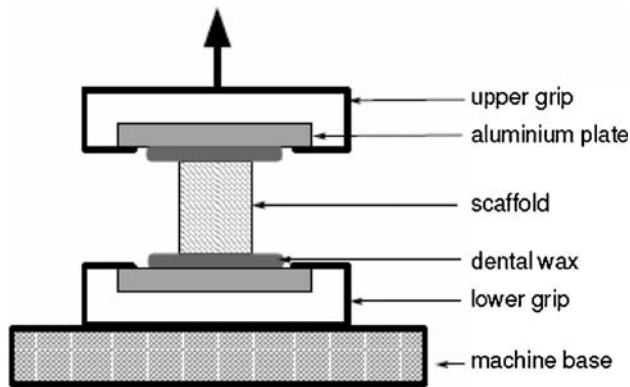
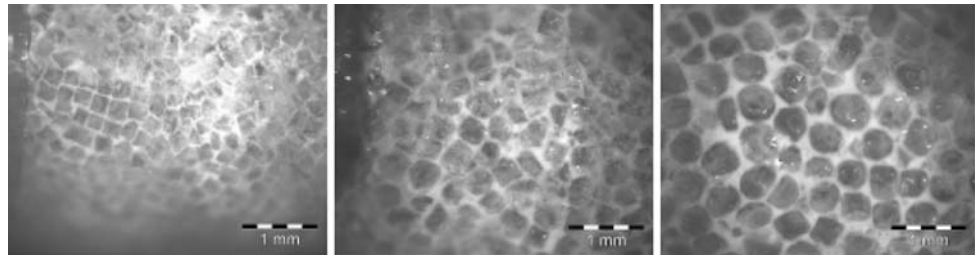


**Fig. 2** Schematic of the tensile tests. The scaffold is in the centre attached via epoxy resin to aluminium discs, which were held by the upper and lower grips in the machine set-up

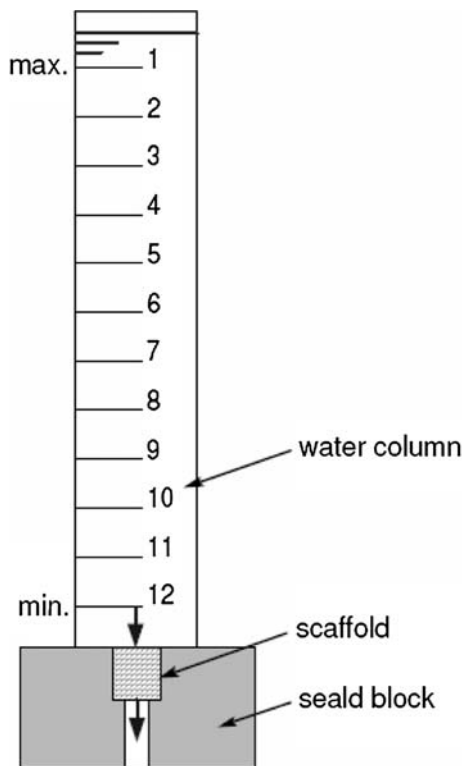


**Fig. 3** Schematic view of the set-up for the experimental permeability tests. The medium flows from the Plexiglas tube through the scaffold in the polyvinyl chloride holder to a beaker

shown in Fig. 3. The device was constructed from a 260-mm long upper Plexiglas tube and a bottom scaffold holder (Fig. 3). An aliquot of 0.9% NaCl was chosen as the medium for permeability in the system. The tube was fixed to the scaffold holder via a press fit connection. The seal of the connection was validated. The scaffold holder was made out of polyvinyl chloride with an inner tube for the scaffold fixation. The inner tube had a diameter of ~6.5 mm to ensure a slight press fit of the scaffolds (diameter 6.8 mm). Time periods between the marks on the Plexiglas tube were measured and the permeability was calculated according to Darcy’s equation (Eq. 1). Darcy’s law states that permeability,  $k$ , can be calculated from the following expression (1) where  $Q$  is the volumetric flow rate (ml/s),  $\Delta P$  is the pressure difference across the sample (N/m<sup>2</sup>),  $l$  is length of the specimen through which the fluid flows (m),  $A$  is the sample cross-sectional area in the direction of flow (m<sup>2</sup>) and  $\mu$  is the viscosity (Pa s) of the fluid.

### 3.2 Mathematical permeability

A mathematical model utilising a tetrakaidecahedral unit according to O’Brien et al. [3] and Gibson and Ashby [6] was used to calculate the permeability of the hyaluronan-collagen scaffolds with three different mean pore sizes. O’Brien et al. [3] have previously shown that cellular solids modelling techniques using a tetrakaidecahedral unit cell can accurately represent and predict salient micro structural features of collagen scaffolds. The tetrakaidecahedron is a polyhedron that packs to fill space, approximates the structural features of many experimentally characterised low-density, open-cell foams, nearly satisfies the minimum surface energy condition, and is often used for modelling such foams [6, 20]. In their investigation a quantitative, cellular solids model describing the permeability ( $k$ ) of collagen scaffolds in terms of scaffold mean pore size ( $d$ ), per cent compression ( $\epsilon$ ), a dimensionless system constant ( $A'$ ), and scaffold relative density ( $\rho^*/\rho_s$ ) has been developed from a series of known cellular solids relationships (Eq. 2).

$$k = A' \cdot \left(\frac{d}{2.785}\right)^2 \cdot (1 - \epsilon)^2 \cdot \left(1 - \frac{\rho^*}{\rho_s}\right)^{3/2} \quad (2)$$

In our investigation the dimensionless system constant  $A'$  was taken from O’Brien et al. [3]. The mean pore sizes

varied as seen in Table 1. No compression of the scaffolds was performed ( $\varepsilon = 0$ ), therefore  $(1 - \varepsilon)^2$  was set as 1. The density  $\rho^*$  of the scaffolds was measured prior to the tests (Eq. 3).

$$k = A' \cdot \left(\frac{d}{2.785}\right)^2 \cdot 1 \cdot \left(1 - \frac{\rho^*}{\rho_s}\right)^{3/2} \quad (3)$$

### 3.3 Porosity

The scaffolds were weighed using a digital scale (Mettler Toledo, PB 153-S, Switzerland; accuracy of 0.1 mg). The individual dimensions of the scaffolds were measured using a Microscope (Olympus SZX12 with camera colour view 12) with the resolution of 50:1. The density of the scaffolds was calculated using weight and volume of each individual scaffold (Eq. 4). Equation 5 was used to calculate the theoretical density of a 30% collagen and 70% hyaluronan compound. The relative density of the scaffolds was then calculated using the density of each scaffold and the theoretical collagen-hyaluronan density (Eq. 6). The individual porosities of the scaffolds were calculated using Eq. 7 [6].

$$\rho_{\text{scaffold}} = \left(\frac{\text{weight}_{\text{scaffold}}}{\text{volume}_{\text{scaffold}}}\right) \quad (4)$$

$$\rho_{\text{coll/hyaluronan}} = 0.3 * \rho_{\text{coll}} + 0.7 * \rho_{\text{Hya}} \quad (5)$$

$$\rho_{\text{relative}} = \left(\frac{\rho_{\text{scaffold}}}{\rho_{\text{coll/hyaluronan}}}\right) \quad (6)$$

$$\text{porosity} = 1 - \rho_{\text{relative}} \quad (7)$$

### 3.4 Statistical analysis

Data are reported as the mean  $\pm$  SD. One-way analysis of variance with Tukey post-hoc tests for multiple comparisons

was performed using SPSS Software for Windows Version 12.0.1. Significance was set at a level of  $P < 0.05$ .

## 4 Results

### 4.1 Tensile tests

The rupture stress of the three different scaffold types is shown in Fig. 4a. Figure 4b includes the Young's Moduli of the scaffolds in tension according to their mean pore sizes. Increasing pore sizes showed significantly increased values for rupture stress and Young's Modulus comparing the scaffold with the smallest (302.5  $\mu\text{m}$ ) and the largest (525  $\mu\text{m}$ ) mean pore size. No change in the strain at rupture could be seen between the three analysed scaffolds.

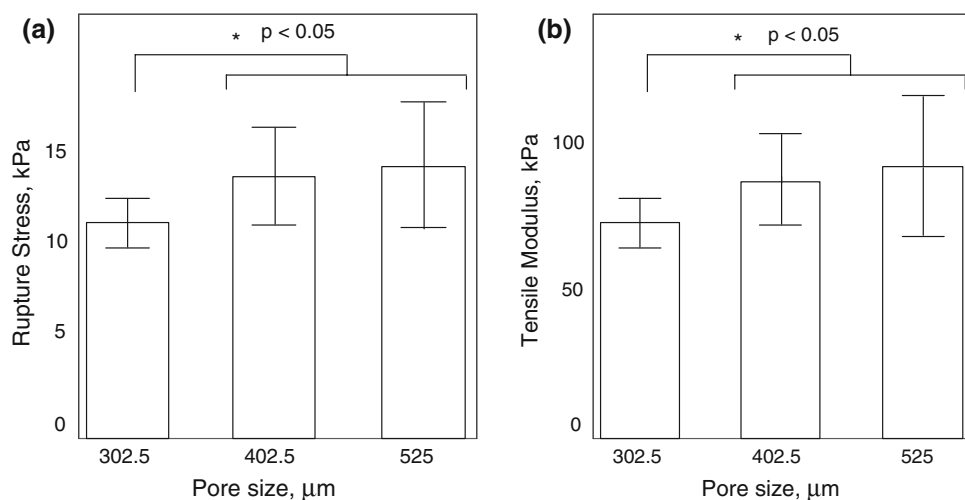
### 4.2 Permeability

The experimentally measured and mathematically calculated permeability values with deviations as a function of pore size are shown in Fig. 5. Increasing pore sizes showed significantly increased values for permeability comparing the scaffold with the smallest (302.5  $\mu\text{m}$ ) and the largest (525  $\mu\text{m}$ ) mean pore sizes. The mathematical model showed similar results. However no significant difference could be observed comparing the experimental and mathematical model.

### 4.3 Porosity

The experimentally measured porosity of the collagen-hyaluronan scaffolds as a function of pore size is shown in Fig. 6. The scaffold types with mean pore sizes of 302.5 and 402.5  $\mu\text{m}$  showed both a porosity of 94%. The scaffolds with the largest pore sizes (535  $\mu\text{m}$ ) showed a

**Fig. 4** (a) Rupture stress and (b) Tensile Moduli of the three different scaffolds ( $n = 10$ ) as a function of their mean pore sizes



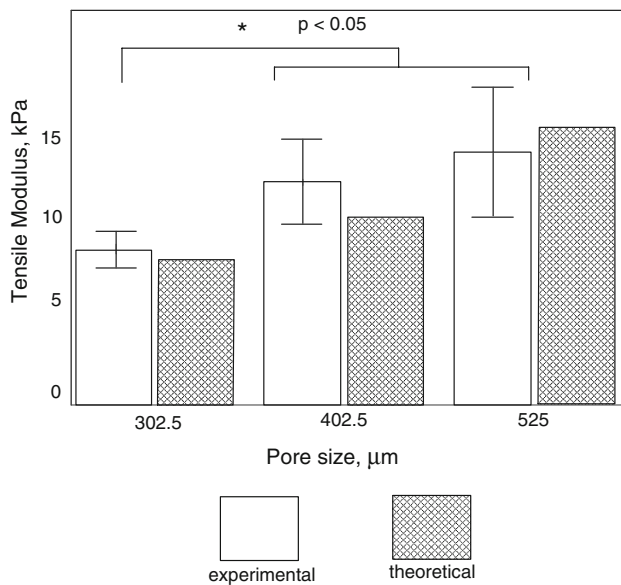


**Fig. 5** Permeability *K* of the three different scaffolds (*n* = 10) as a function of their mean pore sizes

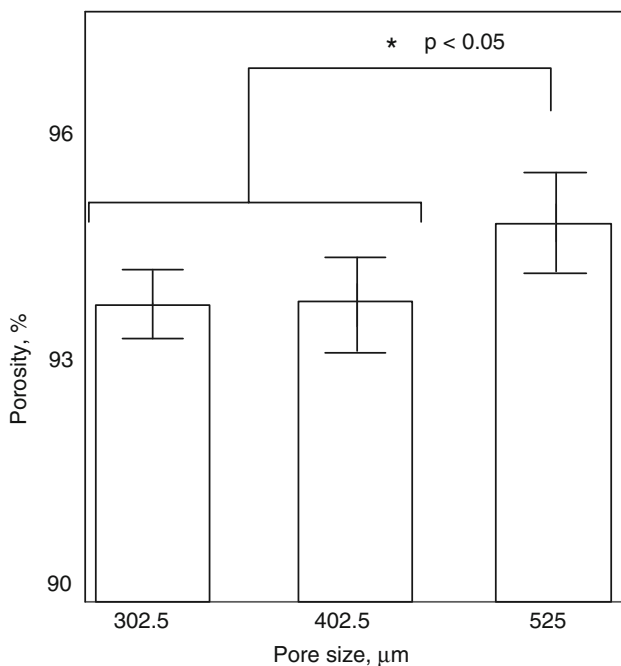


**Fig. 6** Porosity of the three different scaffolds (*n* = 10) as a function of their mean pore sizes

statistical significantly higher porosity of 95%. However, in an overall aspect, this higher porosity seems negligible.

**5 Discussion**

The aim of this study was to investigate the effect of pore size on the mechanical properties, permeability and

porosity of hyaluronan-collagen scaffolds. With increasing pore sizes an increasing rupture stress, as well as increasing Young’s Moduli, could be seen. The same effect was seen in the permeability and porosity. Taken together the results indicate an important influence of pore size on mechanical stiffness, permeability and porosity.

Pore size plays a significant role in TE, as it affects an individual cell’s response in terms of cell attachment, growth and proliferation [5, 7]. Variation in pore size also influences the mechanical stability of the constructs (Fig. 4) which is important for implanting the constructs in load bearing areas, as well as to evaluate the construct response to mechanical stimuli in bioreactors.

Permeability and porosity of scaffolds is important in TE as it controls the migration of cells into the 3-D construct as well as in nutrient and waste transport. The influence of permeability has been studied in various biological materials as bone [21], tumour tissue [22, 23], cartilage [24] and collagen scaffolds [3]. It has been reported that permeability of cartilage tissue [24] and collagen scaffolds [3] is dependent on the mechanical loading, and therefore the strain of the construct. Scaffold permeability also influences cyclical changes in biophysical stimuli due to fluid flow during mechanical loading in bioreactors caused by compression [17], hydrostatic loading [17] or flow perfusion [3]. In particular permeability affects the magnitude of pressure and fluid shear stresses within the construct or tissue, both of which have been identified as potential stimuli for cellular differentiation or functional adaptation [25, 26]. Construct permeability has also been shown to influence the degradation rate of biodegradable scaffolds for TE [27]. Increasing the mean pore size from 302.5 to 525 µm showed a significantly increased porosity and permeability of the hyaluronan-collagen scaffolds. Porosity and permeability are highly connected and therefore the results correlate. By increasing the scaffold pore size the fluid has more space to flow through the matrix and the Darcy’s constant increase (Eq. 1) [3]. The device designed to measure the permeability of hyaluronan-collagen scaffolds was adapted from literature [3]. Extrapolating these results, a similar trend compared to O’Brien et al. [3] using collagen glycosaminoglycan scaffolds could be indicated. O’Brien et al. [3] compared the experimental measured values for the permeability with a mathematical model with a good correlation ( $R^2 = 0.9956$ ) between the experimental and theoretical results. However, in this investigation deviations in the experimental and analytical results could be observed. Set-up artefacts or the presence of a certain not known swelling pressure during the confined condition of the experiment can influence the results, but we assume a nonlinear relation between pore size and permeability in our hyaluronan-collagen scaffolds. Using a salt leaching fabrication

process a special architectural structure is found in our scaffolds. Primary pores caused by the salt crystals are mixed with secondary pores caused by macro and micro cracks during the drying process of the scaffolds. This forms a special interconnectivity of the pore structure in the scaffolds which can cause this deviation to the mathematically model caused results.

The use of different salt crystals in a salt leeching process also influences obviously the structure and pore formation of the scaffold (Fig. 1). Concerning the variation of the used salt crystals not only the size of the pores in the scaffolds changes. The salt crystals with a small grain size assume to produce a scaffold with a cubic structure, while the architecture of the scaffolds produced with the large salt crystals looks spherical (Fig. 1). Also the intermediate wall thickness increases with increasing salt crystals. The same amount of hyaluronan-collagen slurry was used to produce the scaffolds, therefore the measured density of the scaffolds stayed constant with changing the pore sizes. This can also result in a more homogeneous structure of the matrices. Increasing numbers of rough edges in smaller pore size scaffolds can lead to stress localisations and therefore weaken the structure.

Significant differences in the mechanical properties concerning the different pore sizes could be seen in this investigation. Increasing pore sizes showed higher Young's Moduli and rupture stresses in the scaffolds. Both the change from cubical to spherical shapes of the pores as well as the more homogeneous structure when increasing the pore size may be responsible for the higher rupture stress and the Young's Moduli observed in the tensile tests. The sample preparation especially the cutting process results in deviations of length and parallelism of the cylindrical specimen. This leads to tangential deviation of the applied stresses after fixation in the machine set-up. Therefore a non-uniform loading condition is provoked during the tensile tests. In particular this straightening process at the initial tests may lead to increased deviation concerning the Young's modulus.

Recapitulating mechanical properties, permeability and porosity are very important in TE as they control many processes starting with seeding scaffolds with cells, the migration of the cells into the 3-D structures up to resist mechanical loads after the implantation of the constructs into load-bearing areas.

## 6 Conclusion

The biological, mechanical and structural properties of scaffolds play a key role in TE. Hyaluronan-collagen scaffolds have been investigated according to their biological performance for cartilage TE previously [1, 11, 16–19].

Taken together this study investigated successfully the influence of different pore sizes on the mechanical properties, the permeability and the porosity of hyaluronan-collagen scaffolds. While the differences in the porosity were negligible, tensile and permeability tests were highly dependent on varying the pore size.

## References

1. P. Angele, J. Abke, R. Kujat, H. Faltermeier, D. Schumann, M. Nerlich, B. Kinner, C. Englert, Z. Ruszczak, R. Mehrl, R. Mueller, *Biomaterials* **25**, 2831–2841 (2004)
2. X. Bai, Z. Xiao, Y. Pan, J. Hu, J. Pohl, J. Wen, L. Li, *Biochem. Biophys. Res. Commun.* **325**, 453–460 (2004)
3. F.J. O'Brien, B.A. Harley, M.A. Waller, I.V. Yannas, L.J. Gibson, P.J. Prendergast, *Technol. Health Care.* **15**, 3–17 (2007)
4. E.B. Hunziker, *Osteoarthr. Cartil.* **10**, 432–463 (2002)
5. F.J. O'Brien, B.A. Harley, I.V. Yannas, L. Gibson, *J. Biomater.* **26**, 433–441 (2005)
6. L. Gibson, M.F. Ashby, *Cellular Solids, Structures and Properties.* (Cambridge University Press, Cambridge, 1988)
7. F.J. O'Brien, B.A. Harley, I.V. Yannas, L. Gibson, *Biomaterials* **25**, 1077–1086 (2004)
8. L.J. Chamberlain, I.V. Yannas, H.P. Hsu, G. Strichartz, M. Spector, *Exp. Neurol.* **154**, 315–329 (1998)
9. I.V. Yannas, E. Lee, D.P. Orgill, E.M. Skrabut, G.F. Murphy, *Proc. Natl Acad. Sci. USA* **86**, 933–937 (1989)
10. P. Angele, R. Kujat, U.S. Patent, 2004
11. P. Angele, R. Kujat, M. Nerlich, J. Yoo, V. Goldberg, B. Johnstone, *Tissue Eng.* **5**, 545–554 (1999)
12. L.A. Solchaga, B. Johnstone, J.U. Yoo, V.M. Goldberg, A.I. Caplan, *Cell Transplant.* **8**, 511–519 (1999)
13. B. Johnstone, J. Yoo, *Expert Opin. Biol. Ther.* **1**, 915–921 (2001)
14. M. Koide, K. Osaki, J. Konishi, K. Oyamada, T. Katakura, A. Takahashi, K. Yoshizato, *J. Biomed. Mater. Res.* **27**, 79–87 (1993)
15. D.A. Grande, C. Halberstadt, G. Naughton, R. Schwartz, R. Manji, *J. Biomed. Mater. Res.* **34**, 211–220 (1997)
16. P. Angele, H. Faltermeier, R. Kujat, M. Maghsudi, H.D. Moller, M. Nerlich, *Langenbecks Arch. Chir. Suppl. Kongressbd.* **115**, 205–208 (1998)
17. P. Angele, D. Schumann, M. Angele, B. Kinner, C. Englert, R. Hente, B. Fuchtmeier, M. Nerlich, C. Neumann, R. Kujat, *Biorheology* **41**, 335–346 (2004)
18. P. Angele, J.U. Yoo, C. Smith, J. Mansour, K.J. Jepsen, M. Nerlich, B. Johnstone, *J. Orthop. Res.* **21**, 451–457 (2003)
19. R. Muller, J. Abke, E. Schnell, F. Macionczyk, U. Gbureck, R. Mehrl, Z. Ruszczak, R. Kujat, C. Englert, M. Nerlich, P. Angele, *Biomaterials* **26**, 6962–6972 (2005)
20. W. Thompson, *Phil. Mag.* **24**, 503 (1887)
21. M.L. Knothe Tate, U. Knothe, *J. Biomech.* **33**, 247–254 (2000)
22. P.A. Netti, D.A. Berk, M.A. Swartz, A.J. Grodzinsky, R.K. Jain, *Cancer Res.* **60**, 2497–2503 (2000)
23. C.A. Znati, M. Rosenstein, T.D. McKee, E. Brown, D. Turner, W.D. Bloomer, S. Watkins, R.K. Jain, Y. Boucher, *Clin. Cancer Res.* **9**, 5508–5513 (2003)
24. J.M. Mansour, V.C. Mow, *J. Bone Joint Surg. Am.* **58**, 509–516 (1976)
25. I. Owan, D.B. Burr, C.H. Turner, J. Qiu, Y. Tu, J.E. Onyia, R.L. Duncan, *Am. J. Physiol.* **273**, C810–C815 (1997)
26. P.J. Prendergast, R. Huiskes, K. Soballe, *J. Biomech.* **30**, 539–548 (1997)
27. C.M. Agrawal, J.S. McKinney, D. Lanctot, K.A. Athanasiou, *Biomaterials* **21**, 2443–2452 (2000)